

Image analysis of scanning electron microscope images to determine crack-opening stress, crack shape and strain field of fatigue cracks exposed to overloads

L. Jacobsson¹, C. Persson² and S. Melin³

¹ Division of Materials Engineering, Lund University, Sweden, lars.jacobsson@material.lth.se

² Division of Materials Engineering, Lund University, Sweden, christer.persson@material.lth.se

³ Division of Mechanics, Lund University, Sweden, solveig.melin@mek.lth.se

ABSTRACT. *Fatigue crack propagation rates are affected by the characteristics close to the crack tip. A method is developed to measure the displacements along the crack, close to the crack tip, using high resolution scanning electron microscope images. Images are taken throughout the load cycles to observe the displacements of a crack exposed to one single overload. The potential drop technique is used to measure the electrical contact between the crack surfaces.*

For experiments with $R=0.03$ and ΔK in the mid Paris region and higher, a remaining displacement is detected and both the crack opening and closure loads are decreased after the overload. This leads to an increasing effective stress intensity factor range which results in an initially higher crack propagation rate following the overload.

INTRODUCTION

From the work by Elber [1] in the seventies it is well known that the crack closure level has a pronounced influence on the crack propagation rate. The assumption is that the stresses in the crack tip vicinity become positive at the stress level where the crack opens. From this load, measured globally, and maximum load, an effective stress intensity factor range can be calculated. With this entity, the dependence on stress ratio R can be eliminated, so that the crack propagation rates are the same at same effective stress intensity factor range.

When a fatigue crack is exposed to an overload, the crack opening level is changed and the plastic zone size is increased, and this will influence the crack propagation rate da/dN [2], [3], with a the crack length and N the number of cycles. Under small scale yielding conditions the changes in da/dN are related to variations, through the load cycles, in the crack shape close to the crack tip, and the shape may be affected due to residual stresses, crack surface roughness or other features.

To measure the opening and closure stresses levels, different techniques can be used. The compliance method provides the global load versus displacement, measured e.g. at

a point far from the crack, at the crack mouth, or along the crack path. For this, different types of extensometers, or clip gages [4] are used, or microscope observations [5] made. Another method to measure the crack closure and the crack propagation rate is the potential drop technique [6], [7]. This method measures the electrical potential drop over the crack mouth when a direct current passes through the test specimen.

The aim of this study is to investigate the characteristics of the crack tip displacements continuously during the load cycles for the case of a fatigue crack, exposed to one single overload. An in-situ scanning electron microscope (SEM) technique is used to take high resolution images of the crack tip region, and the images are analyzed with an image analyzing computer program.

EXPERIMENTAL PROCEDURE

In-situ SEM crack propagation experiments were performed on Inconel 718. Single edge notch tension specimens were cut in dimensions of 70 x 10 mm from a 0.5 mm foil. The specimens were prepared with a notch, and a fatigue crack was initiated at sixty percent of the yield stress and with $R = 0.03$ in a servo hydraulic MTS load frame. When the crack started to propagate the load was lowered, and propagation was continued up to a crack length of about 1 mm. The test specimens were etched and prepared for measurements of the electrical potential drop over the crack mouth resulting from electrical contact between the crack surfaces. Thin wires were welded close to, and on each side, of the crack mouth, and a constant direct current of 0.95A was passed through the test specimen to measure the variation in potential drop during the load cycles. A reference signal was measured in an area far from the crack to compensate for variations in the signal other than related to the crack opening. The prepared specimen was placed within the SEM vacuum chamber to be continuously observed in-situ during the load cycles, which were provided by an electrically driven load cell. With this technique high resolution SEM images of the crack tip region could be taken at different applied load levels. The images were analyzed to define the crack opening displacement at different distances behind the crack tip.

To automate the image analyzing process, a computer program was designed to detect shifts in displacements as compared to a reference image, cf. fig. 1. The program uses a cross correlation function that recognizes the same, but displaced, area in different images. These areas were defined at small distances from the crack path, cf. fig 2, which left shows two areas with centres (x_1, y_1) and (x_2, y_2) close to an unloaded crack and right the same two areas in displaced positions with centre points (g_1, h_1) and (g_2, h_2) . It was found that the displacements in the load direction remained constant within a vertical distance of up to 10 μm from the crack faces so the choice of placement of the areas was not critical in the vertical direction.

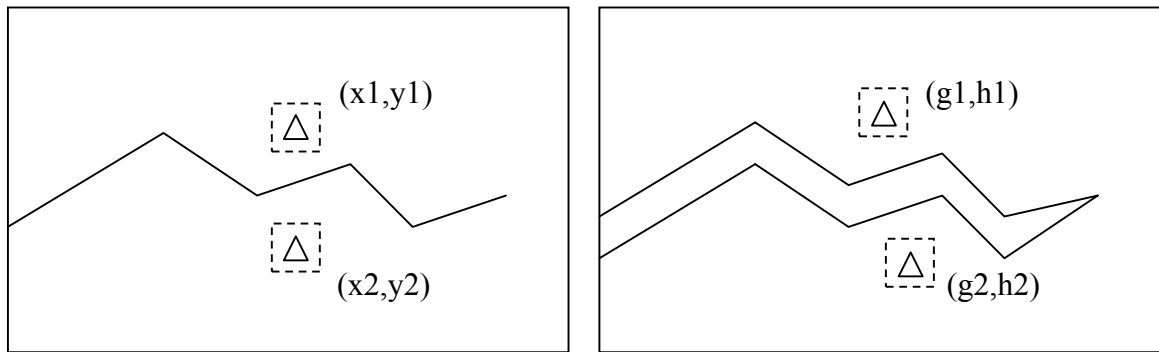


Figure 1. Areas used for cross correlation. Left: unloaded configuration. Right: displaced configuration. Area centre points are marked by Δ . The displacements in the load direction were calculated as $\delta = (h_1 - h_2) - (y_1 - y_2)$.

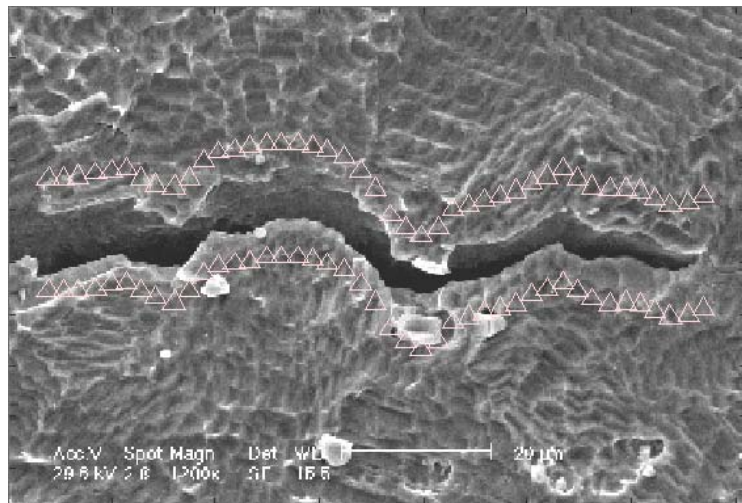


Figure 2. The displacements along the crack were calculated for the area centre points, marked with Δ , cf. fig. 1.

The experiments were run with load cycles with constant applied minimum and maximum loads, resulting in increasing stress intensity factor with increasing crack length. The crack was grown some distance away from the initial notch where after one single overload cycle was applied. The overload cycle, the cycle before it and the one after were observed. Compliance curves were measured at a small distance behind the crack tip from high resolution SEM images taken during the load cycles.

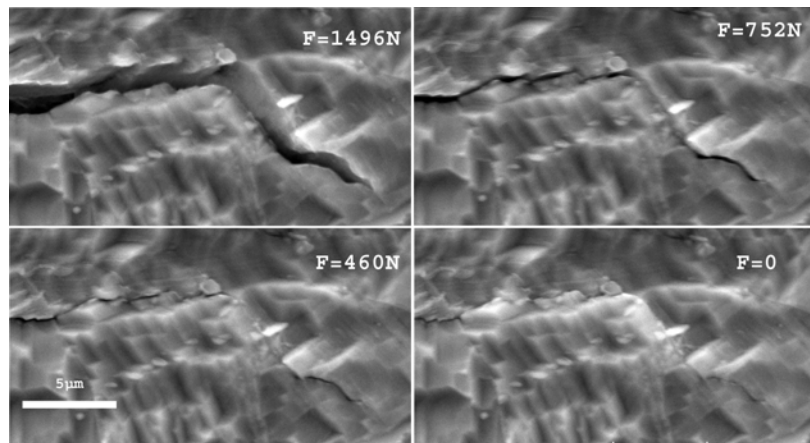


Figure 3. SEM images of the displacements close to the fatigue crack tip during unloading from external load $F_{max}=1496$ N to $F_{min}=0$ N.

RESULTS AND DISCUSSION

Examples of SEM pictures, where the crack is followed during unloading, is seen in fig. 3. At maximum load, $F_{max}=1496$ N, the crack is fully open. During unloading the crack closes from the tip through a zipping behaviour and is fully closed at minimum load, $F_{min}=0$ N. The effects of an overload is illustrated in fig.4 where crack length a as function of number of cycles N is shown. Three overload events can clearly be detected from the curve through jumps in a , at $N=2386$, 3424 and 4230 cycles.

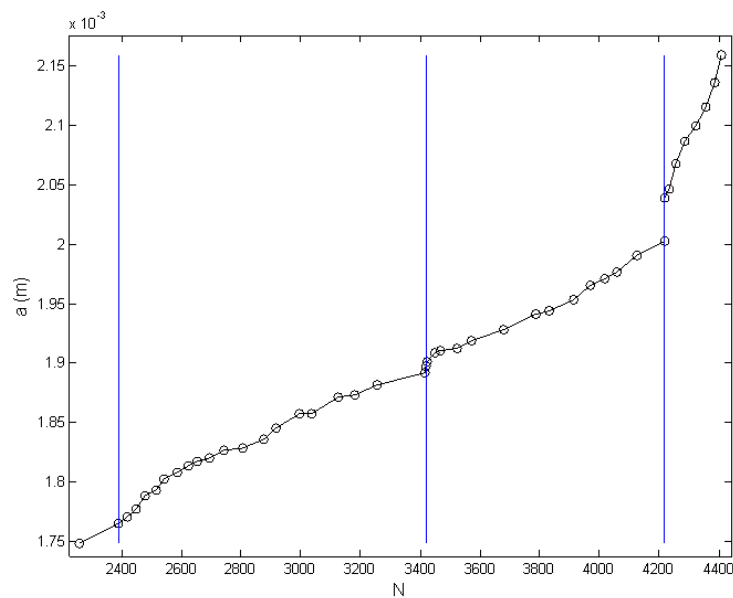


Figure 4. Crack length for a specimen subjected to overloads at $N=2386$, 3424 and 4230 cycles.

Compliance curves were produced from displacements close to the crack tip to include effects from the plastic zone. This effect was obvious in the mid and high Paris regions, with stress intensity factor ranges between 40 and 70 MPa \sqrt{m} and including one single overload cycle. During the overload the plastic zone increased, resulting in a remaining deformation of the crack faces, that separates them up to a distance of 10 μm from the crack tip at zero load. This is seen from the compliance curves in fig. 5 for the overload cycle, the cycle before, and the one after the overload. Figure 5 applies to $\Delta K=65\text{MPa}\sqrt{m}$, $R=0.03$, and $K_{ol}=82\text{MPa}\sqrt{m}$, with K_{ol} denoting the overload stress intensity factor.

The compliance curve after the overload, \square in fig. 5, shows that the opening and closure stresses have lower values as compared to prior to the overload, which gives less crack closure. This results in a higher effective stress intensity factor range, which increases the forces on the material at the crack tip, leading to increasing crack propagation rate directly after the overload.

Observations of the shape of the crack close to the tip during the overload cycle show that at moderate load levels, the crack tip is sharp even during the overload. When the load level is increased, the crack tip starts to blunt due to the large plastic deformations of the grains at the crack tip. These grains are damaged from plastic slip, which results in a crack tip region with numerous sharp micro cracks. The following crack extension starts from one of these micro cracks, and a sharp crack tip is formed through coalescence with the blunted crack tip formed during the overload. There are no remaining displacements in the crack vicinity for the some hundred cycles following the overload.

For every cycle following the overload cycle the opening and closure loads from the compliance curve increase due to increasing length of the sharp crack propagating away from the blunted area. The shape of the compliance curve after the overload gradually approach a shape similar to the one before the overload, but at a higher PD-signal level, i.e. the potential drop is increased due to the increase in crack length.

One characteristic of the potential drop curves is a pronounced knee at high stress intensity factor levels and this provides the level of crack opening and closure loads where the crack surfaces have no electrical contact, cf. fig. 6. This load level is higher than the opening and closure loads measured from the compliance curves. For loads close to the threshold value there is no knee in the PD curve because the crack tip is sharp and there is still electrical contact between the crack surfaces at maximum load. This is in contrast to cracks in the mid and high Paris regions, where the crack opening displacement is larger, and the crack surfaces are electrically separated at maximum load.

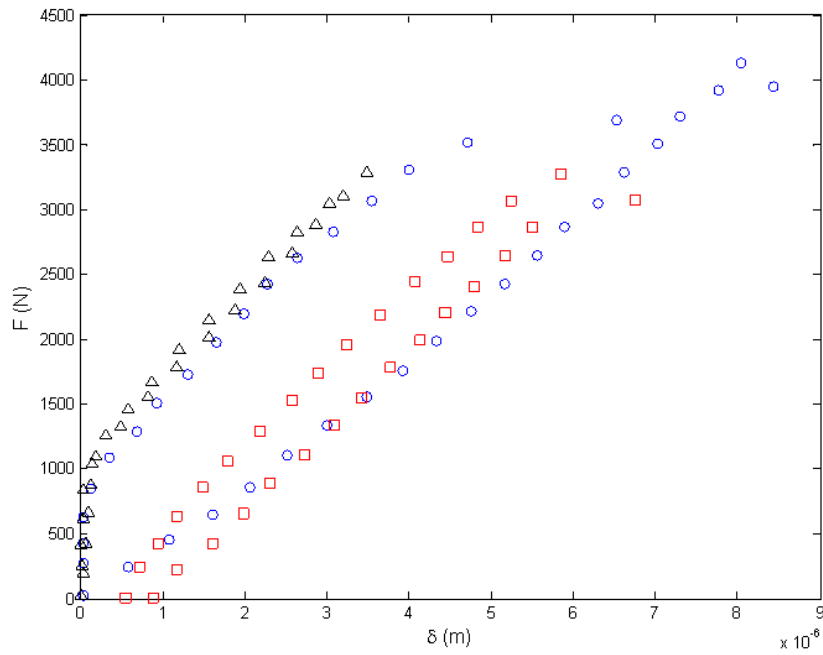


Figure 5. Compliance curves for the cycles before (Δ), during (o) and after (\square) the overload cycle. $\Delta K=65\text{MPa}\sqrt{\text{m}}$, $R=0.03$, $K_{oI}=82\text{MPa}\sqrt{\text{m}}$. For δ , cf. fig. 1.

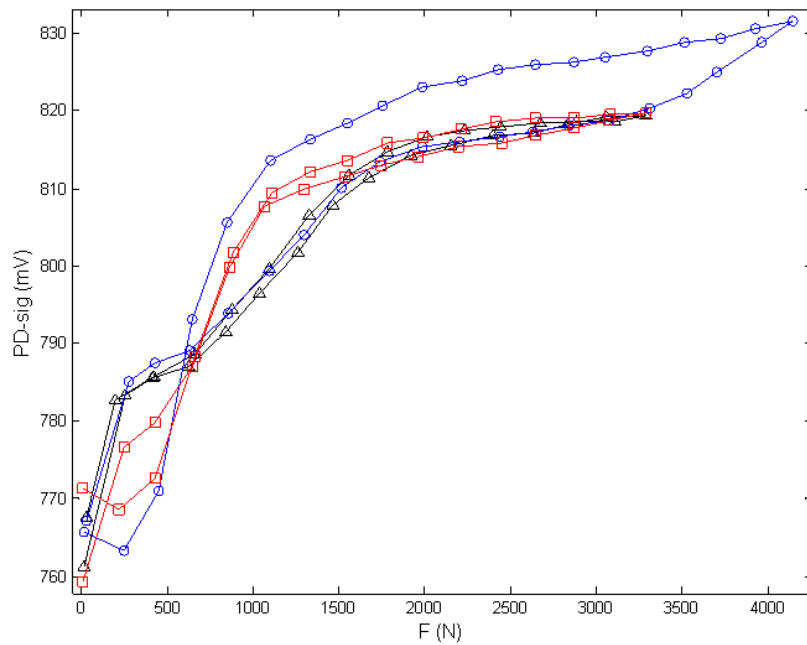


Figure 6. Potential drop signal versus applied load. The curves refer to before (Δ), during (o) and after (\square) the overload cycle. $\Delta K=65\text{MPa}\sqrt{\text{m}}$, $R=0.03$, $K_{oI}=82\text{MPa}\sqrt{\text{m}}$.

CONCLUSIONS

To investigate the mechanisms affecting the crack propagation rate an image analyzing technique was developed to measure the displacements close to the crack tip. Compliance curves were obtained from the measured displacements, and crack opening and closure loads determined for different load sequences.

It was found that the shape of a compliance curve is affected by the plastic zone close to the crack tip, even at small scale yielding.

At potential drop measurements knees during loading as well as during unloading give distinct levels of crack opening and closure. For the mid Paris region, the crack tip was found to be sharp and electrical contact between the crack surfaces, even at maximum load, was observed.

The compliance curves show lower values of crack opening and closure levels than the potential drop measurements. This is because the compliance curve is based on the plasticity influenced displacements close to the crack tip whereas the potential drop technique is based on the electrical contact between the crack surfaces along the full crack length.

When the crack is exposed to one single overload cycle, plastic deformations that remain for many cycles are formed. The crack opening and closure levels decrease, and the propagation rate increases due to a higher effective stress intensity factor.

ACKNOWLEDGEMENT

To the Swedish Gas Turbine Centre for financial support and to Mr. Z. Zivcovic for valuable assistance during the development of the experimental equipment.

REFERENCES

1. Elber, W., *Eng. Fract. Mech.*, 2, 37-45, 1970
2. Shimojo, M., Chujo, M., Higo, Y., Nunomura, S., *Int. J. Fatigue*, vol. 20, no. 5, 365-371, 1998
3. Halliday, M.D., Zhang, J.Z., Poole, P., Bowen, P., *Int. J. Fatigue*, vol. 19, no. 4, 273-282, 1997
4. ASTM, E 399-83, Philadelphia, 1983.
5. Halliday, M.D., Poole, P., Bowen, P., *Fatigue and Fracture of Engineering Materials and Structures*, vol. 18, 717-729, 1995
6. Andersson, M., Persson, C., Melin, S., *ICF 9*, 2003
7. Evans, W.J., Spence, S.H., *Int. J. Fatigue*, vol. 19, no. 1, 205-210, 1997